EXAMINING METALLIC GLASS FORMATION IN LaCe:Nb BY ION IMPLANTATION

by

Richard SISSON, Cameron REINHART, Paul BRIDGMAN, and Tatjana JEVREMOVIC*

Nuclear Engineering Program, University of Utah, Salt Lake City, Ut., USA

Scientific paper
http://doi.org/10.2298/NTRP1702127S

In order to combine niobium (Nb) with lanthanum (La) and cerium (Ce), Nb ions were deposited within a thin film of these two elements. According to the Hume-Rothery rules, these elements cannot be combined into a traditional crystalline metallic solid. The creation of an amorphous metallic glass consisting of Nb, La, and Ce is then investigated. Amorphous metallic glasses are traditionally made using fast cooling of a solution of molten metals. In this paper, we show the results of an experiment carried out to form a metallic glass by implanting 9 MeV Nb 3+ atoms into a thin film of La and Ce. Prior to implantation, the ion volume distribution is calculated by Monte Carlo simulation using the SRIM tool suite. Using multiple methods of electron microscopy and material characterization, small quantities of amorphous metallic glass are indeed identified.

Key words: implantation, metallic glass, niobium, lanthanum, cerium, Monte Carlo

INTRODUCTION

A combination of elements lanthanum, cerium, and niobium in an amorphous metallic glass is investigated using the method of ion implantation and results discussed in this paper. Due to the high melting point of Nb, common methods of metallic glass formation such as melt spinning [1] and physical vapor deposition [2] are not adequate to produce a metallic glass when combined with La and Ce. Ion implantation is therefore investigated as a method of producing thin-film metallic glass. Manageable processes for the production of thin films of La-Cne as mischmetal utilized as the target material exist. Using Nb as an ion projectile circumvent creates a need to achieve the high melting temperature that is required for bulk processing.

Ion implantation is a materials engineering process by which ions of a material are accelerated by an electric field and impacted into a solid. This process is used to change the physical, chemical, or electrical properties of the solid. Ion implantation is commonly used in semiconductor device fabrication, metal finishing, as well as various other applications in materials science research. The implanted ions alter the elemental composition of the target (if the ions differ in composition from the target). Implanted ions also cause many chemical and physical changes in the target by transferring their energy and momentum to the electrons and atomic nuclei of the target material. This causes a structural change in the crystal structure of the target which can be damaged or even destroyed by the energetic collisions. Because the ions have masses comparable to those of the target atoms, target atoms are knocked out of place. If the ion energy is sufficiently high (usually tens of MeV) to overcome the Coulomb barrier, nuclear transmutation can occur, resulting in small quantities of short-lived isotopes.

Ion implantation is used for the modification of target material composition, structure or properties by ballistic interaction with a projectile ion. An ion implantation system consists of an ion source which produces the desired projectile ion at low energies, an accelerator which magnetically or electrostatically accelerates the ion to a higher energy, and a target chamber where the projectile ions impact the target substrate [1]. In this respect, ion implantation is a form of particle radiation. The ions generated by the ion source are typically single atoms or molecules, which means the amount of ions that are implanted in the target is the time-integrated ion current, normally referred to as the dose [2]. A typical beam current obtainable with ion implantation is on the order of microamperes and so the dose, which can be achieved in a reasonable amount of time, is usually less than 10^{22} atoms per cm^2 [3].

Typical ion energies for ion implantation are in the range of 10 keV to 100 MeV. Energies in the range of 10 keV to 100 keV are generally used for surface modification of targets using noble gases which result in a penetration within the nanometer range [2].

* Corresponding author; e-mail: tjevremovic@gmail.com

Higher energy ions will penetrate deeper while producing structural damage to the target and the ions will be distributed more broadly through the target, reducing the peak ion density.

The ion charge state, energy and mass, as well as target composition, determine the maximum range of ions in the target. Ion ranges can be obtained from nanometers up to hundreds of micrometers by adjusting the ion beam parameters. Ions moving through a solid gradually lose their energy by collision with target atoms and from electrostatic drag produced by the overlap of electron orbitals. The loss of ion energy in the target is called stopping power and is calculated using the binary collision approximation method [3].

Basic properties of Nb, La and Ce of interest for their combination into a metallic glass are outlined in tab. 1.

Niobium is mostly used as an alloying element for steel, accounting for 90 % of global Nb consumption [4]; Nb becomes a superconductor at 9.2 K, the highest critical temperature of an elemental superconductor [5]; Superconductive magnets are made with Nb-Zr wire which retains its superconductivity in strong magnetic fields, [6]. Niobium alloy superconducting magnets are used in magnetic resonance imaging, nuclear magnetic resonance instruments, and particle accelerators [7, 8]. Thousands of pounds of Nb are used in advanced air frame systems, like the Gemini space program and Apollo Lunar Modules, [6]. For example, C-103, composed of 89 % niobium, 10 % hafnium and 1 % titanium, is used for liquid rocket thruster nozzles on lunar modules, [9].

Lanthanum has very active chemical properties; new cut metal quickly oxidizes in the air [10]. Compounds are used mainly as additives to glass or crystals to increase durability or to modify absorption and emission. La (III) oxide is added to camera and telescope lenses due to its high refractive index and low dispersion [11]. Lanthanum hexaboride crystals are used in thermionic electron emission sources for electron microscopes and hall-effect thrusters [12]. Mischmetal is an alloy consisting of about 50 % cerium, 25 % lanthanum, 15 % neodymium, and 10 % other rare earth metals and iron. Since the early 1900's, it is the primary commercial form of mixed rare earth metals. Alloyed with iron, it is the flint in cigarette lighters and similar devices, [13]. Fluid catalytic cracking (FCC) is an important conversion process used in petroleum refineries. It is widely used to convert high-molecular weight hydrocarbon fractions of petroleum crude oils to valuable gasoline and other products, [14-16]. Lanthanum-rich rare earth compounds are used extensively as components in FCC catalysts, [17]. LaNi5 hydrogen storage alloys are used in the vehicular battery industry, due to their high hydrogen solubility and capacity of hydrogen absorption and desorption at room temperature. In most cases, mischmetals are used instead of pure La for economic reasons, [18].

Table 1. Properties of Nb, Ce and La

	Melting point [23] [°C]	Crystal structure [23]	Atomic radius [23] [Å]*	Valency [23]
Nb	2.468	BCC	0.690	2-5
La	921	D-HCP	1.061	3
Ce	799	HCP	1.034	3, 4

*1 Å $= 10^{-10}$ m

Cerium is the second most reactive rare metal; it oxides rapidly in air, [6]. It is the major ingredient in mischmetals, used as flint in cigarette lighters and catalysts for the cracking of petroleum, [13, 19]. Ceria is the most widely used compound of cerium. It is used mainly as a polishing compound for the production of high-quality optical surfaces, [20], and widely utilized as a promoter in three-way catalysts for the elimination of toxic exhaust gases, low-temperature water-gas-shift reaction, and oxygen sensors, [21]. Cerium compounds are used to increase the photostability of heavily light or electron- bombarded surfaces. One study found a considerable increase in photostability of Ce-modified titanium dioxide, compared with the unmodified one [22].

Formation of metallic alloys in examining possibility for Nb, La, and Ce to combine

In order to combine Nb, Ce, and La into an alloy, the Hume-Rothery rules need to be followed:

– 1st rule states that the radius of the solute atoms needs to be within 15 % of each other. The percent radii difference required to form an alloy is calculated using the following relation [24]

$$\text{radii difference} \quad \frac{r_{\text{solute}} r_{\text{solution}}}{r_{\text{solution}}} \quad 100\ \% \qquad (1)$$

where r_{solute} is the atomic radius of the metal being dissolved, and r_{solution} is the atomic radius of the solvent metal. Table 1 shows the radii difference for all these three elements, along with other properties important for alloy formation. The cerium atomic radius is 32 % greater than that of La, the Nb radius 28 % less, and the difference between Nb and Ce is 70 %. None of these elements have a radius within 15 %, meaning that the solubility of this mixture is limited.

– 2nd rule states that the elements to be combined need to have a similar crystal structure. The crystal structure of La is double hexagonal close-packed (as shown in tab. 1). Cerium has two crystal structures, the first being double hexagonal close-packed structure and the second being a face-centered cubic form. The niobium crystal structure is a body-centered cubic lattice. Both, Ce and La, therefore, have similar crystal structures and are thus the best candidates to combine into an alloy as long as the Ce is in its hexagonal close-packed structure.

– 3rd rule states that elements with similar valency are more likely to form an alloy. Niobium has a maximum valency of 5, followed by Ce with 4, and La with 3. While the valency is close, these elements probably are not close enough to form a joint alloy.
– 4th electronegativity rule states that atoms with similar enough electronegativity tend to form intermetallic compounds instead of alloys, [24]. Niobium has the highest electronegativity of 1.6, followed by Ce with 1.12 and La with 1.1. Both, Ce and La, have close electronegativity, but Nb differs enough to prevent an alloy from forming and instead form intermetallic compounds. The three elements are different enough that they will not form an alloy easily; that is why amorphous metallic glasses are the only form allowing these three elements to combine.

The benefit that comes from making an amorphous metal instead of a crystalline one is that the material can be engineered to have certain mechanical or electromagnetic properties that cannot be achieved with a crystal structure. For example, amorphous steel which has the unique characteristic of being nonmagnetic and having a low density still provides the necessary material strength. Naval ships or submarines built from this material are less heavy and being nonmagnetic means that mines and traps set off by magnetism will be ineffective against the ship's hull [25]. These materials are made by adding small amounts of rare earth elements like yttrium to disorder the crystal structure. This is similar to how the La-Ce-Nb is made: by displacing the crystal structure of La and Ce by Nb ion implantation, as discussed in this paper.

The ability to form glass-like structures depends on the elements used and in many cases a certain combination can be used to make a metallic glass. When La and Ce are used in conjunction, the elements frustrate the crystal structure so that a metallic glass can be created. Similar elements complicate competing crystalline phases thus disturbing the crystal structure. This means that Ce and La samples can be mixed to form a metallic glass [26].

Adding the transition element Nb to an Al-Ce complex, for example, increases the ductility of the material while still keeping it in an amorphous state. This is also true of adding iron, cobalt, nickel, or copper whereas adding vanadium, chromium, or manganese to the Al-Ce complex only made the material more brittle. Another important property is the crystallization temperature which determines when the structure will change from amorphous to crystalline. From experiments with Al-Ce-M molecules where M stands for Nb, Fe, Co, Ni, and Cu, it was found that increasing the amount of Ce or the amount of M increases the crystallization temperature [27].

FORMATION OF METALLIC GLASSES

Characteristics of metallic glasses

The defining characteristic of metallic glasses is a disordered atomic structure. Typically, metals are crystalline while solid, which is shown by a highly ordered atomic arrangement. Metallic glasses, instead, show an amorphous atomic structure which is non-crystalline. Attaining an amorphous structure in metals is difficult and is normally achieved by liquefying and fast cooling the material [2]. By cooling the metal at hundreds to thousands of degrees per second, the individual atoms are unable to diffuse into a crystal order before losing their thermal energy. In some instances, the temperature required to liquefy the bulk material is difficult to achieve, in which case ion implantation provides an alternative. Ion implantation, as described, is a process by which specific ions are accelerated through an electrical field to impact a solid target material [2]. In the formation of metallic glasses, the projectile ions collide with the underlying crystal structure of the target, causing atomic mixing, introducing a large number of defects and impeding the formation of new crystals. Ion implantation is limited by the energy-range dependence of ion solid interactions where significant particle energies produce limited penetration of the target.

Numerical prediction of the Nb-Ion Implantation for the La-Ce-Nb metallic glass formation

The quality and quantity of metallic glass formed by ion irradiation is heavily dependent on the beam parameters of the ion projectile [28]. Numerical prediction of the radiation-solid interaction is critical to the selection of parameters that will optimize the glass production process.

A high quality LaCe:Nb metallic glass will have uniform distribution of Nb atoms throughout the thin film and a complete absence of single grain crystals and boundaries. A uniform planar (X and Y) distribution of Nb ions is attained by weak focusing of the ion beam producing a Gaussian beam density profile, which is then passed through a set of tantalum masking slits to shape and collimate the beam to an area slightly larger than the target area. Distributing the Nb ions uniformly through the axial direction (Z) is more difficult due to the energy-range dependence of radiation-solid interactions. For one-dimensional calculations, the Bethe-Block equation describes the energy loss of an ion as it moves through an interacting medium [29]

$$\frac{\mathrm{d}E}{\mathrm{d}x} \quad \frac{4\pi z n}{m_e V^2} \quad \frac{e^2}{4\pi\mu_0} \quad ^2 \quad \ln \frac{2m_e V^2}{I} \tag{2}$$

where n [mm^{-3}] is the electron density, z – the charge state, e [C] – the electron charge, μ_0 [Fm^{-1}] – the vacuum permittivity, m_e [kg] – the electron mass, I [eV] – the mean excitation energy, and V [ms^{-1}] – the ion velocity.

Although useful for determining the maximum theoretical range of an ion in a target material, the Bethe-Block equation does not account for the energy-direction relationship that is fundamental to modeling the lateral and axial distribution of ions by inelastic collisions. In order to develop a calculation of the planar and axial deposition of the Nb ions, a Monte Carlo approach can solve the Bethe-Block equation while accounting for changes in direction and energy due to inelastic collisions; this will provide the axial and planar travel through the material. Using this approach, the relationship between ion energy and charge state can be easily explored to determine the best combination of parameters assuring a deposit of ions to be even along the axial direction while minimizing the lateral dispersion.

The actual process of crystal to glass transition is the result of Nb ions colliding and damaging individual La and Ce crystals in a process known as "ion beam mixing" [30]. The efficiency of the ion mixing process is related to the total number of induced displacements per ion (DPA), tab. 2. When examining the Bethe-Block equation, it is possible to infer that a higher charge state will result in more collisions per ion for a given energy. The quantity or, more importantly the rate of metallic glass produced, is time and current dependent. For a Nb irradiation system utilizing a tandem linear accelerator with a 6 MV maximum terminal voltage, the ion beam current is energy and charge state dependent, as shown in fig. 1.

SRIM (Stopping and Range of Ions in Matter) is a computational simulation toolkit for calculating multiple parameters of ion-solid interactions. SRIM can produce quick calculations and tables of stopping powers, range and damage distributions for any ion at any energy in any element or compound target. SRIM is also used to model ion implantation processes, providing information about the kinetic, electronic, and nuclear effects. For the purpose of selecting the best beam configuration to produce metallic glass, SRIM was used to visualize and compare both the final Nb spatial distribution as well as the induced target mixing for multiple beam configurations. Based on the SRIM Monte Carlo simulation of a 3 MeV Nb ion beam in the 2+ charge state, Nb atoms will have shallow penetration with poor dispersion. The Nb atoms will have a high peak density at ~700 nm, fig. 2(a), while the peak damage will occur at ~120 nm, fig. 2(b). The overlap between both the distribution and damage envelopes is very high which is desirable for the formation of glasses, however, the high gradient is undesirable for uniform glass generation. The 8 Mev ion distribution, fig. 3(a), and target mixing, fig. 3(b), show a much higher peak with lower gradient for both parameters. Overlap between the distribution and damage envelopes is also very high, the peak damage is very shallow, while the peak ion density is ~3 m. This profile is more desirable as metallic glass is ex-

Table 2. Summary of SRIM results

Energy [MeV]	Range [m]	DPA
1	0.354	8 660
3	1.030	18 071
5	1.650	23 430
8	2.440	28 494
12	3.350	31 849

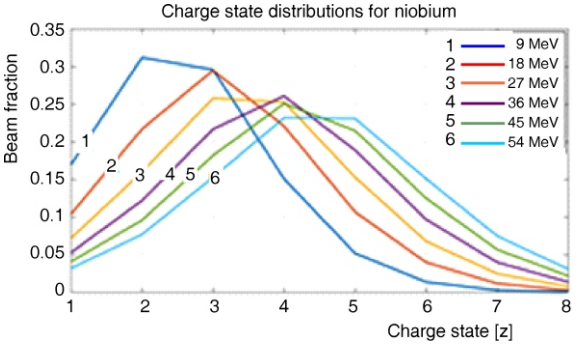

Figure 1. Ion energy and charge state relationship to beam current

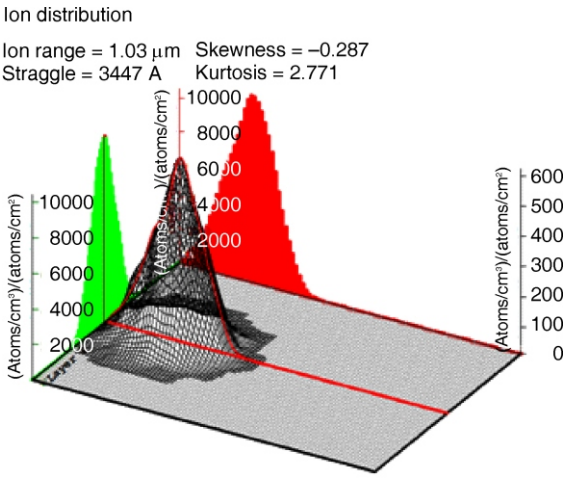

Figure 2(a). 3 MeV Nb distribution in LaCe

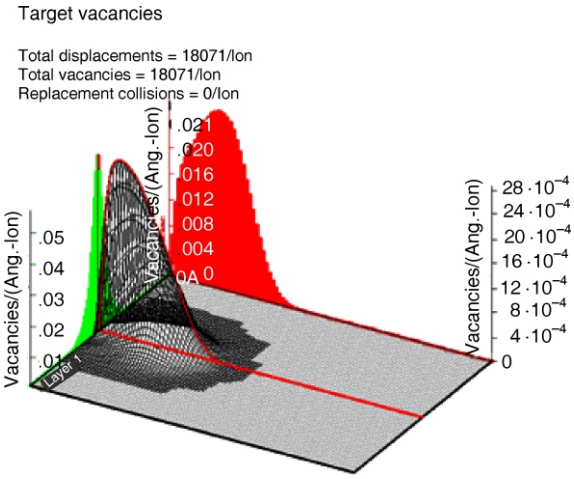

Figure 2(b). LaCe mixing from 3 MeV Nb

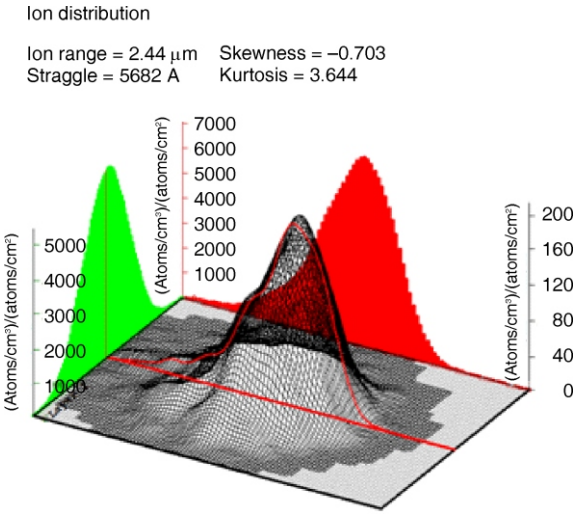

Figure 3(a). 8 MeV Nb distribution in LaCe

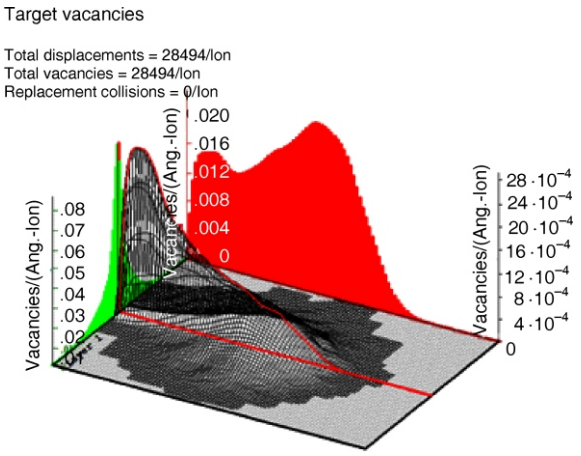

Figure 3(b). LaCe mixing from 8 MeV Nb

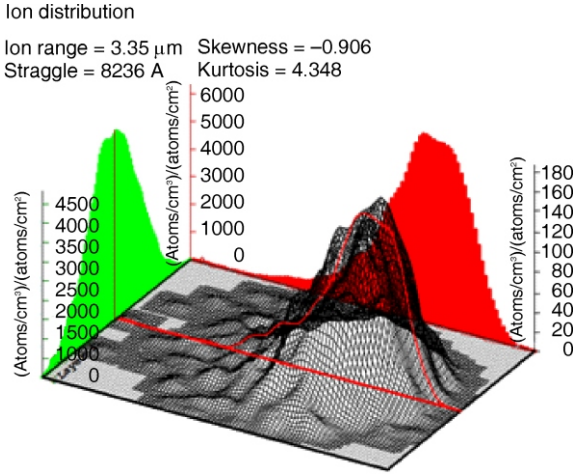

Figure 4(a). 12 MeV Nb distribution in LaCe

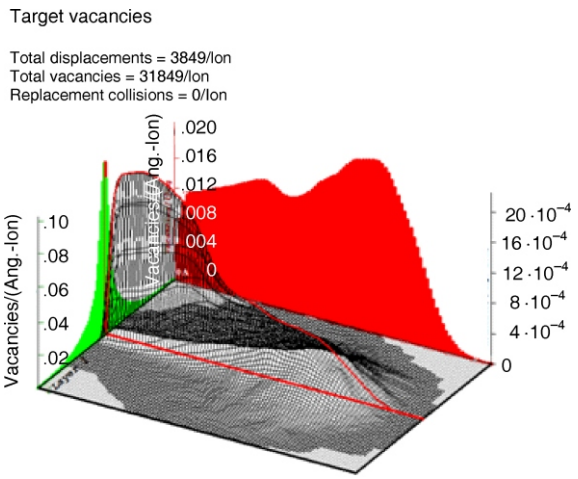

Figure 4(b). LaCe mixing from 12 MeV Nb

pected to form in the shallow region and within the lower concentration shoulders of the profile. The 12 MeV ion distribution, fig. 4(a), and target mixing, fig. 4(b), also produce a higher peak with lower gradient for both parameters. Overlap between the distribution and damage envelopes is also very high, while the peak damage is very shallow. Peak ion density is ~4 m. This profile is also desirable for the formation of metallic glass in the shallow region and within the lower concentration shoulders of the profile.

Selection of beam parameters

The final selection of ion beam parameters is constrained by the time available for accelerator use and the achievable spot size. Based on the known composition of the target, the final composition of the irradiated sample is proposed to include 10 % of Nb. The irradiation time required for deposition is calculated based on the following relations

$$\text{Time} \quad \frac{D}{I_b} \tag{3}$$

where the required ion dose D is

$$D \quad N_p q e \tag{4}$$

The atom quantity N_p is defined as

$$N_p \quad N_e \varepsilon V_t \frac{\rho_t}{A_t} \tag{5}$$

The deposition volume V_t is

$$V_t \quad A_b d_p \tag{6}$$

where I_b is the beam current, q – the projectile charge state, e – the elementary charge, N_e – the Avogadro's number, ε – the molar fraction of projectile, V_t – the target volume, ρ_t – the target density, A_t – the target atomic mass, A_b – the beam spot area, and d_p – the projectile deposition depth.

Table 3. Predicted irradiation parameters for 3 mm spot with +2 Nb Ions at 25 nA

Depth [μm]	Volume [mm^3]	Atoms Nb	Dose [nC]	Time [h]
0.5	0.0035	9.64E14*	3.09E5	3.4
1	0.0070	1.93E15	6.18E5	6.9
1.5	0.0106	2.89E15	9.27E5	10.3
2	0.0141	3.86E15	1.24E6	13.7
2.5	0.0170	4.82E15	1.54E6	17.2

*9.64E14 = 9.64 10^{14}

The resulting values, summarized in tab. 3, show that the energy dependent deposition depth of 0.5 m will result in 9.64 10^{14} Nb ions being deposited in a 0.0035 cubic millimeter volume. The resulting integrated charge dose is 3.09 10^5 nC and will take 3.43 hours to complete. From SRIM, we can determine that a deposition depth between 1.0 and 1.5 μm is achievable using a 3 MeV ion beam that requires ~ 10 hours to complete.

EXPERIMENTAL METHOD

Based on the calculations performed using SRIM as well as the calculated charge state distribution fig. 1, the selected ion beam was configured to produce a 3 MeVNb 2+ beam.

Target preparation

Target samples were used both for analysis and for follow-on experiments. Samples for analysis were prepared on 10 mil steel foils, as shown in fig. 5.

Preparation of the La and Ce precursor consisted of dissolving ~3 g of both cerium/ceria solid and lanthanum/lanthanum oxide solid in 100 mL of dilute Nitric acid. Using an electro-molecular deposition technique, the cerium nitrate and lanthanum nitrate salts were reduced and deposited on the substrates and then the samples were annealed for 5 hours at 720 °C.

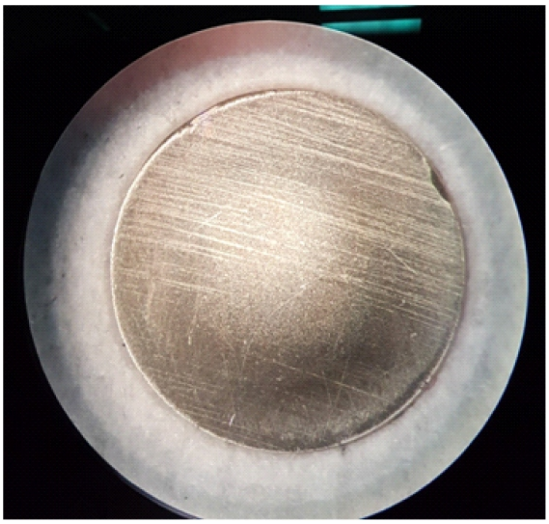

Figure 5. LaCe coupon

Pre-analysis

Before irradiating the samples, the material composition of the sample was confirmed using EDS analysis, fig. 6. The SEM image of the non-irradiated LaCe in fig. 7 shows a mostly homogenous solid metal surface.

SEM imaging in fig. 8 shows that after polishing the surface debris, cracks and fissures were removed without significant modification of the sample surface. EDS composition analysis after polishing shown in fig. 9 shows that the composition was unchanged. The analysis yielded similar results to fig. 6, with the addition of trace amounts of aluminum from the 1 aluminum/alumina oxide polishing slurry used for polishing. Composition was estimated by EDS software and reflected a roughly 50 wt.*% La, 35 w.t.% Ce, 15 w.t.% contaminants, shown in the upper right corner of fig. 9.

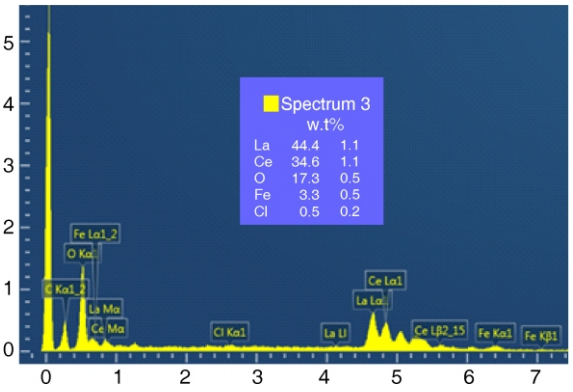

Figure 6. EDS spectrum of a non-irradiated sample before polishing, showing sample composition

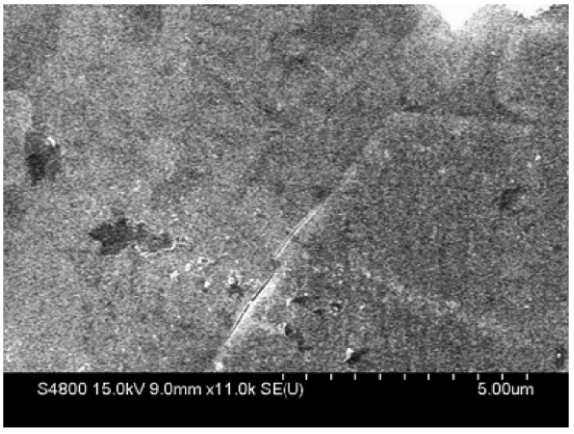

Figure 7. SEM image of non-irradiated sample before polishing

* wt. % means weight percent

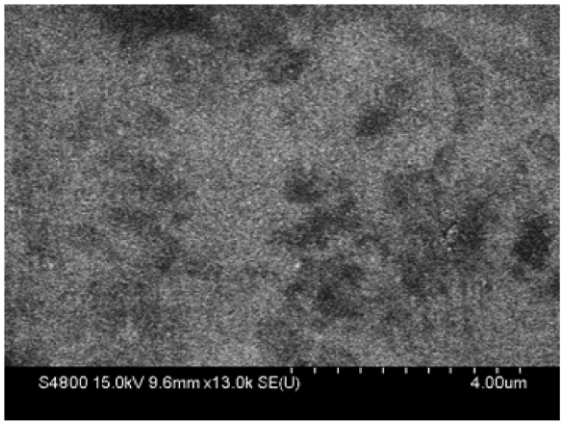

Figure 8. SEM image of non-irradiated sample after polishing

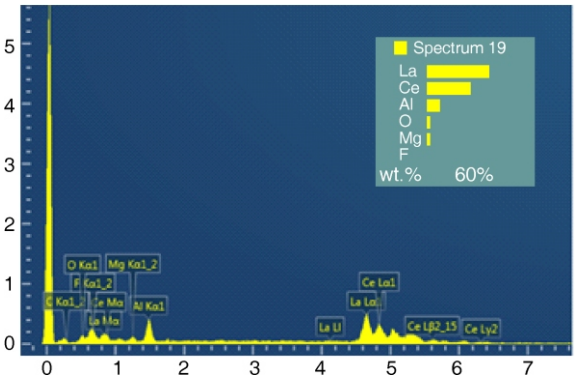

Figure 9. EDS spectrum results from non-irradiated sample after polishing, showing sample composition unmodified by polishing

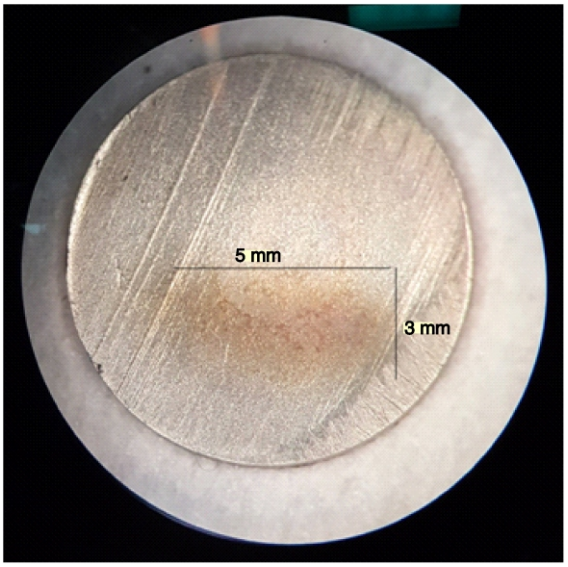

Figure 10. LaCe coupon after Nb irradiation

Table 4. Predicted dose *vs*. measured dose of experiment

Predicted dose [nC]	Measured dose [nC]	Predicted [%] Nb	Measured [%] Nb
$1.97\ 10^6$	$3.97\ \ 10^5$	10 %	0.43 %

Ion irradiation

Irradiation was performed using the 6 MV Tandem Linear Accelerator at Sandia National Lab Ion Beam Laboratory. Niobium negative ions were produced using a SNICS (Source of Negative Ions by Cesium Sputtering) at 54 keV. The negative ions were accelerated into the Tandem accelerator at 1.003 MeV and passed through a nitrogen gas stripper producing Nb ions of multiple positive charge states. The 2 + Nb charge states were selected from the total beam by a 1.54k Gauss analyzing magnet. The 2 + Nb ions were then focused to impact on the sample substrates. The beam current was measured using a Faraday cup and was found to be ~27 nA on the target. The sample was placed in the path of the beam and allowed to be irradiated for ~10.7 hours to produce an on target fluence of $3.95\ 10^{18}$ ions/cm^2. Using a current integrator, the final dose was found to be $3.97\ 10^5$ nC. The measured value was approximately 1/3 of the predicted quantity of Nb atoms from tab. 4. Although lower than expected, the quantity of Nb would be within a measurable range.

Upon the removal of the sample, the beam spot and deposition area were easily visible, as shown in fig. 10. Measurement of the deposition region indicated that the beam was deposited in ~15 mm^2, much larger than the assumed beam spot that informed the dose calculations. Updating the calculation to account for the enlarged beam spot shows a required dose of 1.97E6 nC. The final dose measurement indicates that less than 1 % of the expected quantity of Nb was deposited into the sample.

RESULTS

Irradiation produced the sample shown in fig. 10. The discoloration on the center of the sample shown at 10 magnification in fig. 11 indicates the highest Nb ion deposition and most likely region for metallic glass formation. The samples were viewed using scanning electron microscopy (SEM) and analyzed for metallic content using energy-dispersive X-ray spectroscopy (EDS).

SEM images of the irradiated sample shown in figs. 12(a) and 12(b) revealed large areas of glassy formations. These glassy formations were found only in the discolored ion irradiated region of the sample. The fractured glassy regions indicated increased brittleness of the surface, enhancing the likelihood of metallic glass formation in the Nb irradiated region.

EDS composition analysis was performed on the irradiated sample shown in fig. 13. The composition was estimated by EDS software and reflected a roughly 35 wt. % La, 30 wt. % Ce, 35 wt. % of contaminants, as shown in the upper right corner of fig. 13. Nb was not present in the EDS analysis but the system

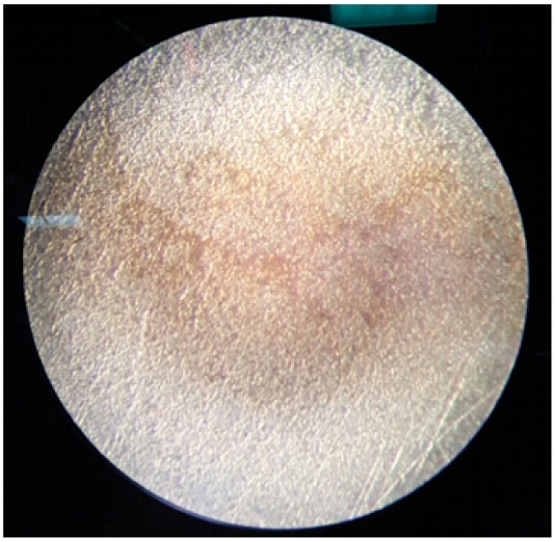

Figure 11. Nb ion irradiated region 10 magnification

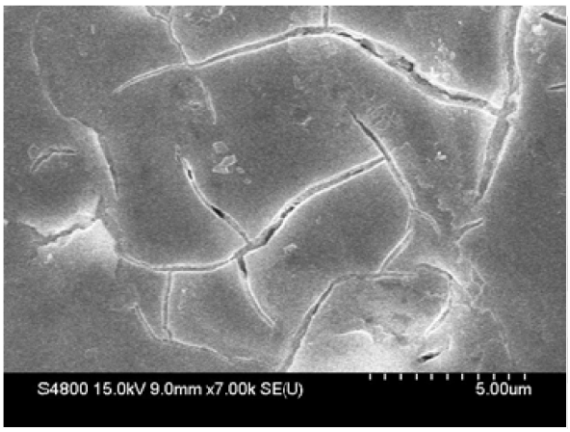

Figure 12(a). SEM image of Nb irradiated region

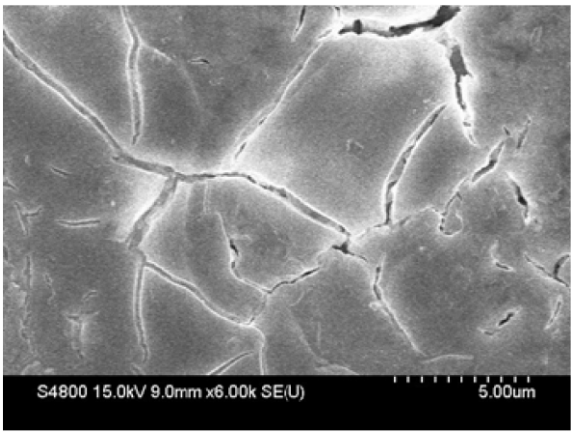

Figure 12(b). SEM image of Nb irradiated region

possessed a lower threshold limit of 1 wt. % composition, much larger than an implantation layer of 4-8 microns. The change in the surface of the metal to the fractured glassy structures indicated the presence of a structural change, likely due to the presence of implanted Nb ions.

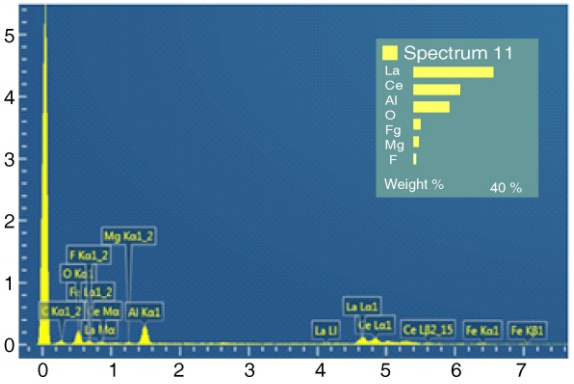

Figure 13. EDS spectrum results from irradiated sample

CONCLUSION

In order to combine elements La, Ce, and Nb, beams of Nb ions were shot into targets made of La and Ce for approximately 30 hours. The targets were made on 10 mil steel foils prepared by electro-molecular depositions of a solution of lanthanum oxide, ceria, and nitric acid onto the foils. Samples were then annealed for 5 hours at 720 °C. SRIM simulations were done in order to find the best energy for firing the ions into the target. It was found that a beam of 2+ Nb ions at an energy of 3 MeV would penetrate the target and place Nb atoms inside. From the EDS analysis, it was found that La and Ce were present in the samples, but that Nb was not. EDS has an error rate of 1 w.t. %, so Nb could still be present since EDS might not be able to detect the 4-8 micron layer of implanted Nb. SEM images taken of the sample show glassy regions that only formed in the Nb irradiated region of the sample. The change from a metallic to a glassy fractured structure was likely caused by the implantation of Nb ions.

REFERENCES

[1] Suzuki, K., Ion Implantation and Activation – Vol. 1. Sharjah: Bentham Science Publishers, 2013, eBook Collection (EBSCOhost), Web, Aug., 27, 2016
[2] Suzuki, K., Ion Implantation And Activation – Vol. 2, Sharjah: Bentham Science Publishers, 2013, eBook Collection (EBSCOhost), Web, Aug., 27, 2016
[3] Suzuki, K., Ion Implantation and Activation – Vol. 3. Sharjah: Bentham Science Publishers, 2013, eBook Collection (EBSCOhost), Web, Aug., 27, 2016
[4] ***, Minerals Yearbook Metals and Minerals 2006 Vol. 52, 2008, US. Geological Survey
[5] Peiniger, M., Piel, H., A Superconducting Nb3Sn Coated Multicell Accelerating Cavity, *Nuclear Science*, 32 (1985), 5, pp. 3610-3612
[6] Elements, 2016, Retrieved from http://periodic.lanl.gov
[7] Glowacki, B. A., *et al*., Niobium Based Intermetallics as a Source of High-Current/High Magnetic Field Superconductors, *Physica C: Superconductivity, 372-376* (2002), 3, pp. 1315-1320
[8] Ciovati, G., *et al*., America's Overview for Superconducting Science and Technology of Ingot Niobium, Melville, NY: American Inst. of Physics., 2011
[9] Hebda, J., Niobium Alloys and High Temperature Applications, Niobium Science & Technology, *Pro-*

ceedings, International Symposium Niobium 2001, Orlando, Fla., USA
[10] Moore, R. J., Lanthanum Compounds, Production and Applications, Hauppauge, N. Y., Nova Science, p. 112
[11] Lide, D. R., ed., CRC Handbook of Chemistry and Physics, 86th ed., CRC Press, Boca Raton Fla., USA, 2005
[12] Sommerville, J. D., King, L. B., Effect of Cathode Position on Hall-Effect Thruster Performance and Cathode Coupling Voltage (PDF), 43rd AIAA/ASME /SAE/ASEE Joint Propulsion Conference & Exhibit, July 8-11, 2007, Cincinnati, O., USA
[13] ***, Misch M., *et al*., 2016, Encyclopedia Britannica, Inc. Retrieved from http://academic.eb.com/levels/collegiate/article/52954
[14] Gary, J. H., Handwerk, G. E., Petroleum Refining: Technology and Economics, 4th ed., 2001, CRC Press., Boca Raton, Fla., USA
[15] Speight, J. G., The Chemistry and Technology of Petroleum, 4th ed., 2006, CRC Press., Boca Raton, Fla., USA
[16] Sadeghbeigi, R., Fluid Catalytic Cracking Handbook, 2nd ed., Gulf Publishing, 2000
[17] Gupta, C. K., Krishnamurthy, N., Extractive Metallurgy of Rare Earths, CRC Press., Boca Raton, Fla., USA, 2004, p. 44
[18] Uchida, H., Kuji, T., Hydrogen Solubility in Rare Earth Based Hydrogen Storage Alloys, *International Journal of Hydrogen Energy, 24* (1999), 9, pp. 871-877
[19] Greenwood, N. N., Earnshaw, A., Chemistry of the Elements, Pergamon Press., Oxford, UK, 1984
[20] Reinhardt, K., Winkler, H., Cerium Mischmetal, Cerium Alloys, and Cerium Compounds., Ullmann's Encyclopedia of Industrial Chemistry, Wiley-VCH, Weinheim, 2000
[21] Qiao, Z., *et al*., Shape-Controlled Ceria-Based Nanostructures for Catalysis Applications, *Chem. Sus. Chem., 6* (2013), 10, pp. 1821-1833
[22] Glen, M., Grzmil, B., Photostability and Optical Properties of Modified Titanium Dioxide, *Pure and Applied Chemistry, 84* (2012), 12, pp. 2531-2547
[23] ***, Thermo-Physical Materials Properties Database IAEA (2010) retrieved 1/19/2010 therpro.hanyang.ac.kr/search/search_map.jsp IAEA Therpro
[24] Hume Rothery, W., Atomic Theory for Students of Metallurgy, The Institute of Metals, London, 1969, (5th ed.)
[25] Stein, B. P., Schewe, P. F., Amorphous Steel. Physics Update, *Physics Today, 57* (2004), 8, p. 11
[26] Zhang, T., *et al*., Effect of Similar Elements on Improving Glass Forming Ability, *Journal of Alloys and Compounds*, *483* (2008), 1-2, pp. 60-63
[27] Inoue, S., *et al*., New Amorphous Alloys With Good Ductility in Al-Ce-M (M = Nb, Fe, Co,Ni or Du) Systems, *Japanese Journal of Applied Physics*, *49* (1988), 8, pp. 1796-1799
[28] Narayan, H., *et al*., Surface Smoothing of Metallic Glasses by Swift Heavy Ion Irradiation, *Nuclear Instruments and Methods in Physics Research Section B: Beam Interactions with Materials and Atoms, 156* (1999), 1-4, pp. 217-221
[29] Sigmund, P., Particle Penetration and Radiation Effects, Berlin: Springer, 2006
[30] Clark, G., *et al*., Ion-Beam Mixing in Silicon and Germanium at Low Temperatures, *Nuclear Instruments and Methods in Physics Research*, 1983, pp. 209-210, 107-114. doi:10.1016/0167-5087(83)90788-3

Received on December 12, 2016
Accepted on April 4, 2017

Ричард СИСОН, Камерон РАЈНХАРТ, Пол БРИЏМАН, Татјана ЈЕВРЕМОВИЋ

ИСПИТИВАЊЕ ФОРМИРАЊА МЕТАЛНОГ СТАКЛА ИМПЛАНТАЦИЈОМ ЈОНА НИОБИЈУМА У ЛАНТАНЦЕРИЈУМ

Да би се комбиновао ниобијум са лантанијумом и церијумом, јони ниобијума депонују се на танак филм ова два елемента. Према правилима Хјум-Ротерија, ови елементи не могу се комбиновати у традиционалном облику кристалног метала. Стога је испитана могућност стварања аморфног металног стакла од ниобијума, лантанијума и церијума. Аморфна метална стакла традиционално се праве брзим хлађењем раствора истопљених метала. У овом раду приказани су резулатати спроведеног експеримента ради добијања металног стакла имплантацијом јона атома Nb^{3+}, енергије 9 MeV, у танак филм од лантанијума и церијума. Пре имплантације, применом Монте Карло симулације посредством програмског пакета СРИМ, израчуната је запреминска расподела јона. Вишеструком применом методе електронске микроскопије и карактеризације материјала, заиста је идентификована мала количина аморфног металног стакла.

Кључне речи: имплантација, метално стакло, ниобијум, лантанијум, церијум, Монте Карло метода